

USE OF ADJACENT KNOT DATA IN PREDICTING BENDING STRENGTH OF DIMENSION LUMBER BY X-RAY

Jung-Kwon Oh

Postdoctoral Fellow
Department of Forest Sciences
Seoul National University
Seoul, Korea

Kwang-Mo Kim

Research Scientist
Department of Forest Products
Korea Forest Research Institute
Seoul, Korea

*Jun-Jae Lee**

Professor
Department of Forest Sciences
Seoul National University
Research Institute for Agriculture and Life Sciences
Seoul, Korea

(Received April 2009)

Abstract. In a previous study, the knot depth ratio (KDR) evaluation method was proposed to quantify the area of knots in a cross-section. That study reported that bending strength can be predicted by KDR analysis. However, the KDR model did not take into consideration the additional strength reduction caused by adjacent knots. It was found that the prediction of lumber strength was improved when adjacent knots were taken into consideration. Analysis using the KDRA (KDR adding knots) model revealed that the optimum cross-sectional interval, an input variable, is directly affected by knot size parallel to lumber length (KSPLL). KSPLL depends on the sawing method and log characteristics, and for species containing large knots, the cross-sectional interval is likely to be extremely wide. This can cause several adjacent small knots to be excluded from the analysis, requiring modification of the KDRA model algorithm. This modification resulted in improvement in the precision of the strength prediction, although the input variable of the cross-sectional interval was not used. The R^2 values obtained using this method were 0.60 and 0.56 for Japanese larch and red pine, respectively.

Keywords: Knot depth ratio, X-ray, KDRA, knot cluster, knot spacing, bending strength, strength prediction, adjacent knot, lumber, grading.

INTRODUCTION

Wood is a natural material with physical and mechanical characteristics that vary widely. To use wood resources for structural purposes, two kinds of mechanical performance, strength and stiffness, should be known and controlled to stay within desirable limits. One of two kinds of mechanical performance is the stiffness of the wood, which can be measured using various nondestructive

techniques such as measurement of wave speed (ultrasonic and stress waves), measurement of the natural frequency of the wood, and the flatwise bending test, among others. However, strength cannot be measured until the lumber fails, and then it cannot be used. Therefore, the strength of lumber should ideally be predicted using nondestructive methods.

Wood strength is affected by various defects such as knots, slope of the grain, and cracks. Among these defects, knots are the most serious,

* Corresponding author: junjae@snu.ac.kr

because they can greatly reduce the strength. In destructive bending tests, failure is caused almost exclusively by knots. Schniewind and Lyon (1971) tested redwood lumber and in 95% of the cases, failure occurred at knots or at the local slope of grain that was mainly related to knots. In Johansson et al (1992), 91% of failures were caused by knots.

Riberholt and Madsen (1979) proposed the weakest section theory for the strength of lumber. This theory assumes that timber is composed of localized weak zones connected by segments of clear wood and that failure is initiated primarily in these weak zones, which are related to the defects previously discussed. These authors also reported that the weakest cross-section corresponds to the largest knot or group of knots. Based on the weakest section theory, it is very important to evaluate the resistance of each section in prediction of lumber strength. Therefore, in this study, we focused on developing a method to predict the resistance of a cross-section containing knots.

The concept of knot area ratio (KAR) is generally used to predict the resistance of cross-sections that contain knots. It has been demonstrated repeatedly that lumber strength is inversely proportional to the maximum KAR, which is defined as the ratio of the knot area to the cross-sectional area. However, because the naked eye can inspect only the external appearance of the lumber, it is very difficult to measure KAR in practice. However, X-rays can easily be used to image internal knots. In previous research (Oh et al 2009), the knot depth ratio (KDR) method was proposed to evaluate the geometric quantity of knots and the transition zone in an X-ray path. Oh et al (2008) reported that X-ray analysis based on the KDR value can be used to predict the bending strength of lumber. Schajer (2001) also reported that the bending strength of lumber can be predicted using X-ray.

In addition to knot area in the cross-section, the location of knots and the spacing between knots also determine the strength of lumber. If

the knot spacing is small, adjacent knots cause stress concentration and additional strength reduction. In most visual grading rules such as the Korean standard rule (KSA 2002) and the Western lumber grading rule (WWPA 2005), knots within 150 mm are regarded as a knot cluster. The sum of the knot sizes is used to determine structural grading. However, Schajer (2001) did not consider the influence of adjacent knots on prediction of bending strength using X-ray. In a previous study, Oh et al (2008) proposed a method to add the KDR values of adjacent cross-sections to take into account adjacent knots; this method improved the precision of the bending strength prediction of a Japanese larch specimen. This result indicates that strength prediction models can be improved by considering adjacent knots. However, the model in the Oh et al (2008) study examined only one species, Japanese larch, and is expected to be affected by species, knot size, the spacing between knots, and so on. Therefore, additional studies of other species containing knots of different sizes and spacings are required.

The main objective of this study was to improve the previous algorithm to consider adjacent knots in strength prediction through the use of X-ray.

MATERIALS AND METHODS

Materials

In this study, 121 Japanese larch (*Larix kaempferi*) specimens and 145 red pine (*Pinus densiflora*) specimens were obtained from commercial mills. Japanese larch specimens have many small-sized knots, whereas red pine specimens generally have a small number of large-sized knots. The specimen sizes were 38 mm thick by 140 mm wide by 3.6 m long, and they were kiln-dried to an average MC of approximately 18%.

Experiments

X-ray imaging. An image intensifier (Thales image intensifier TH9429) was used to take

X-ray images of the lumber. The images were taken with X-rays passing through a thickness of 38 mm. The resolution of the X-ray digital images was 2.7 pixels/mm.

Bending tests. After capturing the X-ray images, a static bending test was performed on the same specimens following the methodology of ASTM D198. Because of the uniform moment in third-point bending, no shear stresses act on the lumber when determining the design value, making this an ideal test. However, the number of knots in the Japanese larch specimens was too great to evaluate the resistance of specific knots. Because of the large number of knots, failure occurs in a complex manner and the failure location can be ambiguous. Therefore, center-point loading tests were carried out for the Japanese larch specimens, and the cross-section containing the knot of interest was placed under the loading point. For the red pine specimens, because the failure location could be clearly identified, the third-point bending test was performed to locate the cross-section containing the knot of interest between the two loading points. The test span of the Japanese larch specimens was 2.4 m, whereas the test span of the red pine specimens was 3.0 m. The test speed for both tests was 10 mm/min. Modulus of rupture (MOR) was calculated based on the bending test results. Because only data from specimens that failed at the knot of interest were considered, 97 pieces of Japanese larch and 133 pieces of red pine were analyzed.

Analysis

Basic model for strength prediction. A knot X-ray image and a clear X-ray image were prepared for all specimens by applying the knot detection algorithm (Oh et al 2009) to the raw X-ray image. KDR values were calculated for every pixel of the knot X-ray image according to Eq 1 (Oh et al 2009).

$$KDR = \frac{\rho - \rho_c}{\rho_k - \rho_c} \quad (1)$$

where

KDR = Knot depth ratio (KDR)

ρ = Density for a pixel within the knot X-ray image

ρ_c = Average clear part density obtained by converting the clear X-ray image for the same specimen into a density

ρ_k = Average knot density, which was determined experimentally for Japanese larch (950 kg/m³) and red pine (930 kg/m³)

Based on the KDR calculation, the knot geometry of a cross-section can be predicted as the simplified knot geometry, as shown in Fig 1c. Based on the simplified knot geometry, I_k/I_g for the cross-section of interest can be calculated following Eq 2 (Oh et al 2008). The relationship between MOR and the I_k/I_g value was investigated for the two species.

$$I_k/I_g = \frac{\sum_{i=1}^n \left(\frac{KDR_i \times t \times k^3}{3} + KDR_i \times t \times k \times h_i^2 \right)}{\frac{t \times h^3}{12}} \quad (2)$$

where

I_k = Moment of inertia for the simplified knot geometry

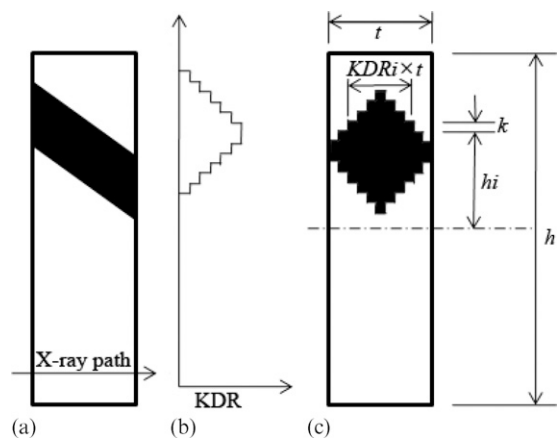


Figure 1. Simplified knot geometry according to the knot depth ratio (KDR) method (Oh et al 2009). (a) Geometry of a real knot. (b) KDR value obtained by X-ray radiation. (c) Simplified knot geometry.

I_g = Moment of inertia for gross cross-section
 KDR_i = KDR value of i^{th} cell
 h = Width of the lumber
 t = Thickness of the lumber
 n = The number of cells in the width of lumber
 k = Width of a cell
 h_i = Distance between the center line and the bottom of the i^{th} cell

Consideration of adjacent knots by the previous model. The KDRA model (KDR adding knots) (Oh et al 2008), referred to in this study, was used to take adjacent knots into consideration. In this model, knots within 150 mm of one another were regarded as adjacent knots (Fig 2a). In an X-ray image, a knot can be placed on several cross-sections, because knot size is generally larger than the unit pixel size of the X-ray image. Initially, among the cross-sections within 150 mm of the knot, $150/k$ sheets of the cross-section were selected with a k mm interval (Fig 2a). To consider the influence of knot spacing, the KDR array of the selected cross-section was multiplied by a triangular weighing function (Eq 3; Fig 2a), and the weighted KDR array of the selected cross-sections was added to the KDR array of the cross-section of interest (Fig 2c; Eq 4).

$$WKDR_i(p) = \begin{cases} \left(1 - \frac{D_p}{75}\right) \times KDR_i(p) & \text{when } D_p \leq 75 \\ 0 & \text{when } D_p > 75 \end{cases} \quad (3)$$

$$KDR_i^* = \sum_p (WKDR_i(p)) \quad (4)$$

where

KDR_i^* = KDR value of the i^{th} cell recalculated by KDRA

$KDR_i(p)$ = KDR value of the i^{th} cell for the p^{th} selected cross-section

$WKDR_i(p)$ = Weighted KDR value of the i^{th} cell for the p^{th} selected cross-section

D_p = Distance between the p^{th} selected cross-section and the interested cross-section (mm)

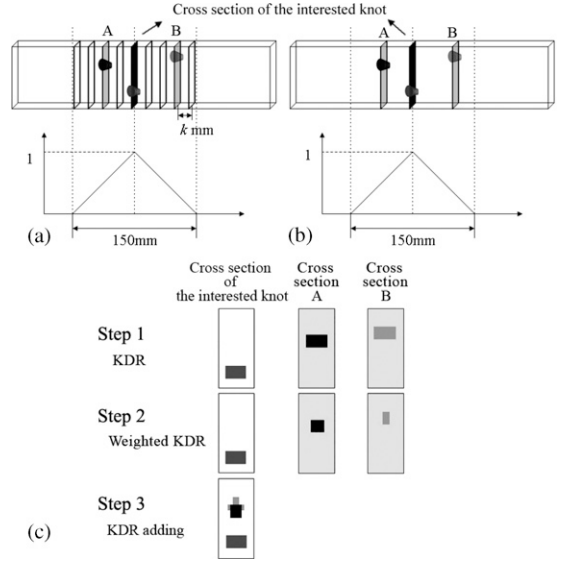


Figure 2. Example of the consideration of adjacent knots. (a) Definition of cross-sections using the knot depth ratio adding knots (KDRA) model and a weighting function (Oh et al 2008). (b) Definition of cross-sections using the modified KDRA model and a weighting function. (c) Work flow for reconstructing cross-sections using these two models.

Some cells of the recalculated cross-sectional array can have values higher than 1.0 because of the addition of the KDR values. Because it is impossible for knot depth to exceed the lumber thickness, we constrained the KDR values of the reconstructed cross-sections to have a maximum possible value of 1.0.

To determine the optimum cross-sectional interval, several intervals of 10 – 50 mm were investigated, and the relationship between MOR and the I_k/I_g values based on the reconstructed KDR values for the cross-sections of interest were evaluated. The coefficients of determination and the root mean square errors (RMSE) were compared to optimize the cross-sectional interval.

The optimum cross-sectional interval was expected to depend on the knot size, in particular, knot size parallel to the length of the lumber (KSPLL, x in Fig 3). A series of knot sizes parallel to lumber length (KSPLL) for a knot were measured along the lumber width (140 mm) for the knot of interest, and average KSPLL for the knots

were calculated. The optimum cross-section intervals were then compared between species. Additionally, the effect of KSPLL on optimum cross-sectional interval was investigated.

Consideration of adjacent knots by the modified KDRA model. In the previous model, cross-sections within 150 mm were selected at intervals that were experimentally determined. In this study, the KDRA model was modified as follows: only one sheet of cross-sections for a knot was selected rather than selecting cross-sections based on cross-sectional intervals. We refer to this model as the modified KDRA model.

Initially, every pixel of the knot X-ray image was investigated using morphological mathematics to determine whether the adjacent pixels were connected to the pixel itself (Fain 2003). The connected pixels were regarded as the area for a knot. Figure 4c shows the identified knot area separated from the other knots; identified knot areas were labeled with numbers.

Among the several cross-sections related to a knot, the cross-section with the maximum I_k/I_g value was selected for each knot (Eq 2; Fig 4d), regardless of knot size, thereby negating the need to use the cross-sectional interval as an input variable. The KDR values of the selected cross-section were added to the KDR value of the interested cross-section after multiplying the KDR array with a triangular weighting function (Figs 2b – c; Eqs 3 and 4). The added KDR values were restricted to have a maximum value of 1.0 as discussed previously. Based on the KDR array of cross-sections reconstructed by adding KDR values, the I_k/I_g value of the cross-section of interest was computed (Eq 2), and the

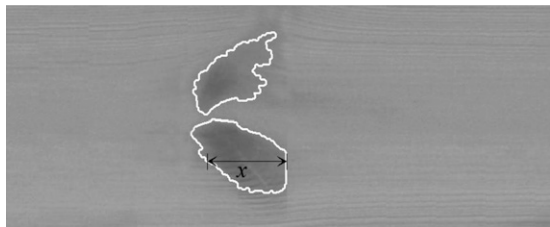


Figure 3. Definition of knot size parallel to the lumber length (KSPLL).

relationship between the I_k/I_g value and the MOR was investigated.

Verification of improvement in the prediction of bending strength. To investigate whether our new model improved bending strength predictions, a one-tailed test with a 10% significance level was carried out. We hypothesized that there were no differences of prediction error between two models. The error was defined as the absolute value of the difference between the MOR predicted by regression analysis and the measured MOR.

RESULTS AND DISCUSSION

Influence of Adjacent Knots on Bending Strength

Figure 5 shows the relationship between the MOR and the I_k/I_g values computed by the basic

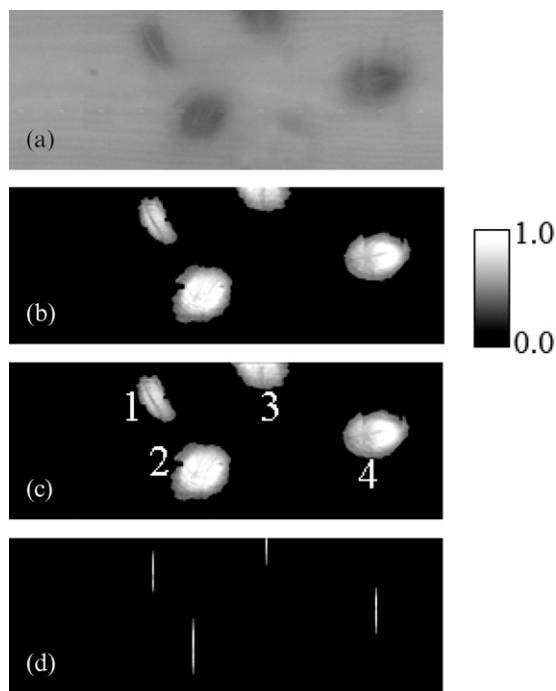


Figure 4. Labeling of knots and selecting cross-sections. (a) Raw X-ray image. (b) Knot depth ratio (KDR) array obtained using the knot detection algorithm and the KDR method. (c) Classification of a knot according to its connectedness. Each classified knot area was labeled with a number. (d) Selected cross-sections.

model. The coefficients of determination (R^2) were 0.49 and 0.45 for Japanese larch and red pine, respectively.

However, regression analysis with the specimens not containing any other knots within 150 mm significantly increased the R^2 value of Japanese larch and red pine to 0.55 and 0.56, respectively (Fig 6). Thus, the basic model does not accurately evaluate the strength reduction caused by adjacent knots within 150 mm.

The KDRA Model and the Optimum Cross-Sectional Interval

In the KDRA model, the KDR values of the selected cross-sections within 150 mm are added to the cross-section of interest. As shown in Tables 1 and 2, KDRA with adjacent cross-sections improved the predictive precision compared with the basic model.

For the KDRA model, $150/k$ sheets of cross-sections were selected, and the cross-sectional interval, k , was determined for the two species.

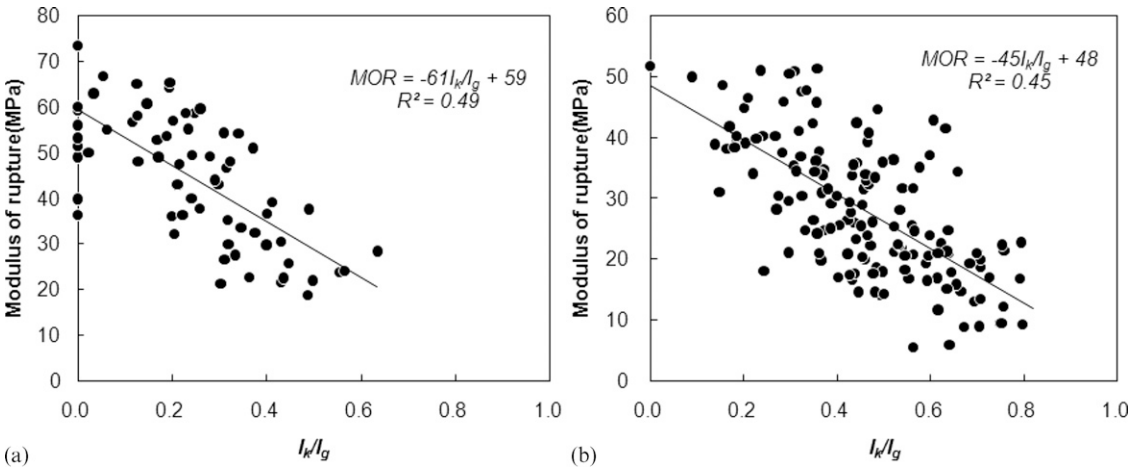


Figure 5. Relationship between the modulus of rupture and the I_k/I_g value according to the basic model. (a) Japanese larch and (b) red pine.

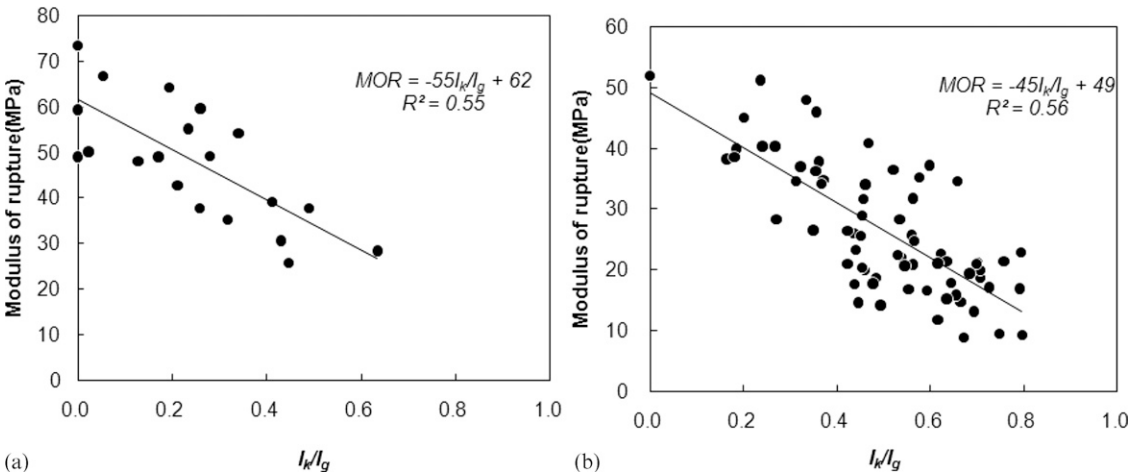


Figure 6. Relationship between the modulus of rupture and the I_k/I_g value according to the basic model for specimens not containing any knots within 150 mm. (a) Japanese larch and (b) red pine.

In Tables 1 and 2, 18 mm and 40 mm showed the strongest relationship and the lowest RMSE for Japanese larch and red pine, respectively. The optimum cross-sectional intervals of the two species are different. To determine the reason for this difference, KSPLL for the knot of interest was measured. Table 3 shows the average KSPLL statistics. The KSPLL of red pine lumber was much larger than that of Japanese larch. The optimum cross-sectional interval of both species was approximately 56% of the average KSPLL.

If the cross-sectional interval were smaller than one-half of the average KSPLL, the knot of

interest was placed onto two or more selected cross-sections (Fig 7a). Too many KDR additions can decrease the predictive precision because excessive additions will result in most KDR values reaching the maximum value of 1.0. If the cross-sectional interval were larger than one-half of the average KSPLL, the knot was placed onto a single selected cross-section. However, if the cross-sectional interval was excessively large, the predictive precision decreased because many small knots were disregarded (Fig 7b).

In the optimum cross-sectional interval analysis, the knot of interest for both species was generally placed on a selected cross-section, because

Table 1. Finding the optimized cross-sectional interval for Japanese larch.

	Cross-sectional interval (mm)	Predictive precision	
		R ²	RMSE
KDRA model	12	0.49	9.9
	14	0.53	9.0
	16	0.57	8.7
	18	0.59	8.6
	20	0.56	8.9
	22	0.51	9.1
	24	0.49	10.0
Basic model		0.49	10.0

RMSE, root mean square error; KDRA, knot depth ratio adding knots.

Table 2. Determining the optimized cross-sectional interval for red pine.

	Cross-sectional interval (mm)	Predictive precision	
		R ²	RMSE
KDRA model	28	0.48	8.2
	32	0.50	8.1
	36	0.52	7.8
	40	0.53	7.6
	44	0.52	7.7
	48	0.51	8.0
	52	0.47	8.2
Basic model		0.45	8.2

RMSE, root mean square error; KDRA, knot depth ratio adding knots.

Table 3. Statistics of the knot size parallel to lumber length (KSPLL) of the knot of interest and the optimum cross-sectional interval in both tree species.

Species	KSPLL		Optimum cross-sectional interval (mm)
	Average	Standard deviation	
Japanese Larch	32.3	16.6	18
Red pine	70.5	36.2	40

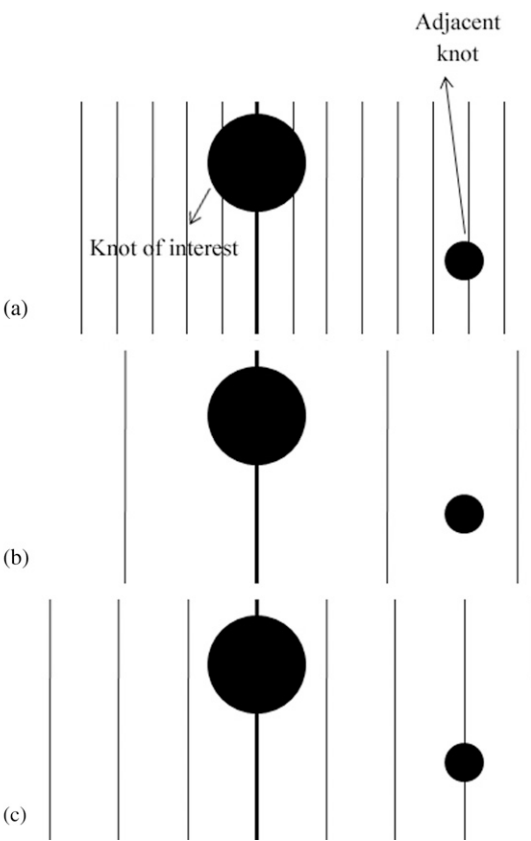


Figure 7. Example of cross-sections according to cross-sectional interval. (a) Excessively wide cross-sectional interval. (b) Excessively narrow cross-sectional interval. (c) Example of an optimal cross-sectional interval.

the optimum cross-sectional interval was slightly larger than one-half of the average KSPLL.

Because the basic model analyzes only one cross-section, knot size perpendicular to lumber length can be considered in I_k/I_g calculation, but KSPLL cannot be analyzed. Adjacent cross-sections are not used in the I_k/I_g calculation. Because the prepared red pine specimens had large knots (KSPLL), it had been expected to require the KDR addition by other cross-sections of the same knot. However, use of a single cross-section for the knot of interest showed the highest predictive precision. Consequently, even if the KSPLL of a knot was large, it was not necessary to add the KDR value of other cross-sections for the knot and only one cross-section for each knot was required.

We also found that the optimum cross-sectional interval was directly affected by the KSPLL. Because the KSPLL depends on the sawing method and the characteristics of the lumber such as the logging site, log diameter, and species, and so on, the optimum cross-sectional interval should be determined whenever the strength is predicted for new batches of lumber. The determination of optimum cross-sectional interval requires a number of failure tests. Frequent determination of it can decrease the feasibility or applicability of the model. Therefore, it is necessary to develop a method that considers adjacent knots without the need to determine the optimum cross-sectional interval in advance.

Additionally, in the case of red pine, the optimum cross-sectional interval was 40 mm. In the

KDRA model, the knots that were smaller than the optimum cross-sectional interval could not be analyzed, but several knots smaller than 40 mm were likely to be present, which was likely to affect the precision of the bending strength prediction.

Prediction of Bending Strength by the Modified KDRA Model

Only one cross-section for a knot was required for the KDRA model regardless of its KSPLL. In the case of species containing large knots such as in red pine, the KDRA model can miss knots smaller than the optimum cross-sectional interval. Based on these findings, the KDRA model was modified.

Improvement of predictive precision by the modified KDRA model. Table 4 shows the results of three different models: basic model, the KDRA model, and the modified KDRA model. For both tree species, the consideration of adjacent knots increased the coefficient of determination and decreased RMSE. Between the two different models for considering adjacent knots, the modified KDRA model showed superior predictive precision.

For red pine, the KDRA model fails to take into consideration knots that are smaller than the cross-sectional interval (40 mm). On the contrary, the modified KDRA model does not require the optimum cross-sectional interval as an input variable, and it can analyze all of the adjacent knots, even if they are smaller than 40 mm. Compared with the KDRA model, the modified

Table 4. Comparison of the modified KDRA model, the KDRA model, and the basic model.

Species	Prediction model	Predictive precision	
		R ²	RMSE
Japanese larch	Basic model ^a	0.49	9.96
	Consideration of adjacent knots	KDRA model ^b	8.57
		Modified-KDRA model	8.42
Red pine	Basic model ^a	0.45	8.16
	Consideration of adjacent knots	KDRA model ^b	7.59
		Modified KDRA model	7.12

^a Basic model: this model does not consider adjacent knots (Oh et al 2008).

^b KDRA model: this model was optimized for each species. Cross-sectional intervals of 18 mm and 40 mm were used for Japanese larch and red pine, respectively.

KDRA, knot depth ratio adding knots; RMSE, root mean square error.

KDRA model increased the predictive precision (R^2 and RMSE), most likely because it takes into consideration knots smaller than 40 mm.

In contrast, the difference in predictive precision between the KDRA model and the modified KDRA model was smaller for Japanese larch than for red pine as shown in Table 4. This is because the cross-sectional interval of 18 mm was small enough to include all of the adjacent knots and the effect of knots smaller than 18 mm tends to be minimal.

To investigate the improvement in the precision of bending strength prediction, a t-test was carried out, and the results are presented in Tables 5 and 6. These results indicate that the KDRA model did not reduce error compared with the basic model; conversely, the predictive error of the modified KDRA model was smaller than that of the basic model at the 10% significance level (H_0 rejected; Table 6). Thus, the modified KDRA model improved the predictive precision.

Both the KDRA and modified KDRA models add the KDR values of adjacent cross-sections to the cross-section of interest. The KDRA model,

however, may be faster than the modified KDRA model because it does not calculate the I_k/I_g values to select a cross-section for each knot. However, the KDRA model requires input of the cross-sectional interval. It was considered that the modified KDRA model would be more applicable because it is not dependent on definition of the cross-sectional interval, assuming that processing capabilities outpace production flow. Additionally, although the modified KDRA model is slower, it provides higher predictive precision, especially in the case of species containing large knots. Figure 8 shows the relationship between the MOR and the I_k/I_g for Japanese larch and red pine.

Optimization of the distance for considering adjacent knots. A distance of 150 mm was used as the range in which to consider adjacent knots in this study. In most visual grading rules such as the Korean Standard (KSA 2002) and Western lumber grading rules (WWPA 2005), knots within 150 mm are regarded as a knot cluster. Although this value has been verified through numerous studies, our model is not intended for visual grading but is instead based on X-ray. Hence, it was necessary to determine a suitable

Table 5. *t*-test results to verify the improvement of predictive precision obtained by using the KDRA model.

		Error		t-test	
		Average ^a	SD ^b	Test statistic	Result ^c
Japanese larch	Basic model	8.29	5.43	1.06	H_0 accepted
	KDRA model	7.49	4.91		
Red pine	Basic model	6.43	5.00	0.80	H_0 accepted
	KDRA model	5.97	4.65		

^a Average error.
^b SD, standard deviation of the error.
^c Result of one-tailed t-test at the 10% significant level.
KDRA, knot depth ratio adding knots.

Table 6. *t*-test results to verify the improvement of predictive precision obtained by using the modified KDRA model.

		Error		t-test	
		Average ^a	SD ^b	Test statistic	Result ^c
Japanese larch	Basic model	8.29	5.43	1.32	H_0 rejected
	Modified KDRA model	7.20	4.28		
Red pine	Basic model	6.43	5.00	1.50	H_0 rejected
	Modified KDRA model	5.62	4.35		

^a Average error.
^b SD, standard deviation of the error.
^c Result of one-tailed t-test at the 10% significant level.
KDRA, knot depth ratio adding knots.

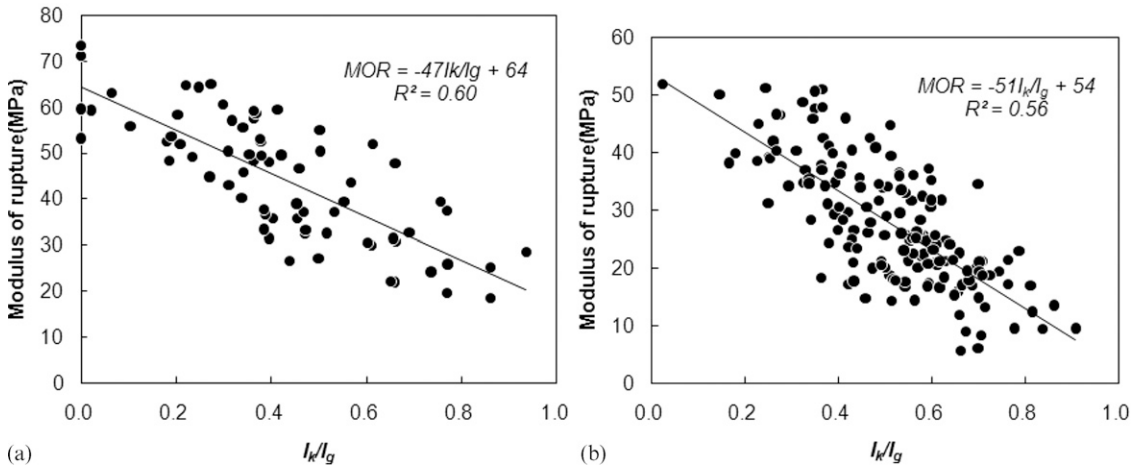


Figure 8. Relationship between the modulus of rupture and the I_k/I_g value according to the modified knot depth ratio adding knots model. (a) Japanese larch and (b) red pine.

Table 7. The predictive accuracies according to the distance used for consideration of adjacent knots.

Distance for considering adjacent knots (mm)	Japanese larch		Red pine	
	R^2	RMSE	R^2	RMSE
50	0.57	8.68	0.43	8.12
90	0.58	8.59	0.51	7.78
110	0.59	8.53	0.53	7.41
130	0.60	8.48	0.56	7.18
150	0.60	8.42	0.56	7.12
170	0.60	8.52	0.55	7.21
190	0.58	8.60	0.46	7.78
220	0.56	8.78	0.36	8.74

RMSE, root mean square error.

distance in which to consider adjacent knots. Several distances over 50 – 220 mm were evaluated. Table 7 shows the predictive accuracies according to distance. Because the knot sizes of red pine are much larger than that of Japanese larch, the optimum distance for considering adjacent knots had been expected to be much larger in red pine than in Japanese larch. However, this distance was similar between the two species (Table 7). Based on this finding, we concluded that distance is not sensitive to knot size. Importantly, a distance between 130 – 170 mm shows a relatively high predictive precision in both species. Thus, 150 mm appears to be a reasonable distance to use for consideration of adjacent knots.

CONCLUSIONS

This objective of this study was to improve the algorithm used to predict bending strength by considering adjacent knots.

Using the KDRA model, the optimum cross-sectional interval was found to be approximately 56% of the KSPLL for both tree species. When the optimum cross-sectional interval was used, the KDRA values for only one cross-section were required for a knot regardless of knot size (KSPLL).

The KDRA model requires input of the optimum cross-sectional interval. However, the optimum cross-sectional interval is related to the size (KSPLL) of a knot, and knot size can vary according to the sawing method used and the log characteristics. Additionally, in the case of species containing large knots, the optimum cross-sectional interval is expected to be too large to evaluate all adjacent knots. This can cause low resolution and therefore low predictive precision.

Based on these findings, we modified the KDRA algorithm to take adjacent knots into consideration. The modified KDRA model was more accurate than the KDRA method, especially for bending strength predictions in red pine, which

has large knots. This modified KDRA model improved the predictive precision of bending strength of $R^2 = 0.60$ for Japanese larch and 0.56 for red pine without requiring the cross-sectional interval as an input variable.

ACKNOWLEDGMENTS

This study was carried out with a grant from the Forest Science and Technology Projects (Project No. S120709L100110) funded by the Korean Forest Service.

REFERENCES

- Fain AK (2003) Fundamentals of digital image processing. Prentice Hall.
- Johansson CJ, Brundin J, Gruber R (1992) Stress grading of Swedish and German timber. A comparison of machine stress grading and three visual grading systems. Swedish National Testing and Research Institute. SP Report 1998:38.
- KSA (2002) Softwood structural lumber, Korean Standard Association, KS F 2162.
- Oh JK, Kim KM, Lee JJ (2008) Development of knot quantification method to predict strength using X-ray scanner. J Korean Wood Sci Technol 36(5):33 – 41.
- Oh JK, Shim K, Kim KM, Lee JJ (2009) Quantification of knots in dimension lumber using a single X-ray radiation. J Wood Sci 55(4):264 – 272.
- Riberholt H, Madsen PH (1979) Strength of timber structures, measured variation of the cross sectional strength of structural lumber. Report R 114, Struct Research Lab, Technical University of Denmark.
- Schajer GS (2001) Lumber strength grading using X-ray scanning. Forest Prod J 51(1):43 – 50.
- Schniewind AP, Lyon DE (1971) Tensile strength of redwood dimension lumber. II. Prediction of strength values. Forest Prod J 21(8):45 – 55.
- WWPA (2005) Western lumber grading rules. Western Wood Products Association, 05:14.3 – 148.